ELSEVIER

Journal of Wind Engineering
and Industrial Aerodynamics 67&68 (1997) 253–265

JOURNAL OF
wind engineering
AND
industrial
aerodynamics

Aeroelastic analysis of bridge girder sections based on discrete vortex simulations

Allan Larsen[a,*], Jens H. Walther[b]

[a] *COWI, 15 Parallelvej, 2800 Lyngby, Denmark*
[b] *Danish Maritime Institute, Hjortekærvej 99, 2800 Lyngby, Denmark*

Abstract

Two-dimensional viscous incompressible flow past bridge girder cross-sections are simulated using the discrete vortex method. The flow around stationary cross-sections as well as cross-sections undergoing cross-wind vertical (bending) and rotary (torsional) motions are investigated for assessment of drag coefficient, Strouhal number and aerodynamic derivatives for application in aeroelastic analyses. Good to excellent agreement with wind tunnel test results is demonstrated for analyses of forced wind loading, flutter wind speed and vertical vortex-induced response of four practical girder cross-sections. The success of the simulations is attributed to the bluff nature of the cross-sections and to the two-dimensional (2-D) nature of flow around bridge girders.

Keywords: Computational bridge aerodynamics; Aeroelastic instability; Buffeting response; Vortex-induced response; Discrete vortex method

1. Introduction

Structural analysis has seen an explosive development during the past 20 years, moving from linear quasi 3-D modal analysis to full 3-D finite element analysis allowing for non-linear effects and complex boundary conditions. A full dynamic analysis of a bridge structure can now be completed within a week, but acquisition of necessary aerodynamic data from wind tunnel section model testing remains quite time consuming. Typical time consumption for planning, model construction, testing and reporting related to wind tunnel testing of a bridge cross-section is of the order of 6–8 weeks.

* Corresponding author. E-mail: aln@cowi.dk.

0167-6105/97/$17.00 © 1997 Elsevier Science B.V. All rights reserved.
PII S0167-6105(97)00077-9

Experience gained from a number of bridge design projects has demonstrated that the time consumption associated with wind tunnel testing of bridge decks puts aeroelastic analyses on the critical path. Reduction of the turn-over time for aeroelastic analyses is thus highly desirable not only from an economical point of view. More important is that a reduction in the turn-over time allows more analyses to be performed within a given budget. The authors have taken up this challenge by developing a relatively fast computer technique based on the discrete vortex method for evaluation of aeroelastic actions on bridges.

The present paper discusses application of the discrete vortex method in aeroelastic analyses of practical bridge girder sections and presents comparisons between numerical simulations and wind tunnel test results. In a companion paper, Walther and Larsen [1] elaborate theoretical aspects of the discrete vortex method (computer code DVMFLOW), developed for bridge aerodynamic applications and discuss the fundamental case of the "flat plate" stationary and in oscillatory motion.

2. Aeroelastic analysis of flexible bridges

Aeroelastic analysis of flexible bridge structures traditionally combines structural dynamic analyses with aerodynamic data derived from wind tunnel model tests. In the analysis 3-D structural properties (mode shapes and structural inertia) are combined with 2-D aerodynamic information assuming conventional "strip theory" to be valid.

An aeroelastic analysis covering the most important design aspects includes horizontal girder response to mean wind and atmospheric turbulence, critical wind speed for onset of flutter and vortex-induced response. Such analyses involve the following 2-D aerodynamic data for the girder cross-section under consideration:

- Drag coefficient C_D: forced horizontal wind response.
- Flutter derivatives $H^*_{1..4}, A^*_{1..4}$: critical wind speed for onset of flutter.
- H^*_1 and Strouhal number St: vertical vortex-induced response.

A detailed discussion of aeroelastic response analyses is offered by Simiu and Scanlan [2].

3. Discrete vortex method for 2-D bridge sections

A distinct feature of flow past bluff bodies, stationary or in motion, is the shedding of vorticity in the wake which balances the change of fluid momentum along the body surface. Similar shedding of vorticity occurs in the wake of streamlined (airfoil-like) bodies in transient motion in a potential flow. The vorticity shed at an instant in time is convected downstream but continues to affect the aerodynamic loads on the body.

Analytical treatment of potential flow past streamlined bodies (e.g. the "flat plate") assumes that the vortical wake is shed from a single point – the trailing edge. The shed vorticity is convected downwind with the speed of the surrounding fluid. This simplified model is not valid for viscous flows past stationary or moving bluff bodies.

As a consequence of viscosity and presence of separation zones the unsteady vortical wake of a bluff body will be shed, not at the trailing edge, but along the entire body contour. Shed vorticity is convected by local mean wind speed and velocity fluctuations associated with viscous diffusion. Shed vorticity will also interact in the wake forming coherent structures – the well-known von Kàrmàn vortex trail. A realistic flow model for bluff bodies was developed within the framework of the "discrete vortex method" and programmed for computer by one of the authors for his Ph.D. Thesis [3]. The resulting numerical code DVMFLOW establishes a 2-D "grid free" time marching simulation of the vorticity field equation. Details of theory and governing equations are presented in a companion paper [1].

The input to DVMFLOW simulations is a boundary panel model of the bridge section contour. The output of DVMFLOW simulations comprises time-progressions of surface pressure distributions and section loads (drag, lift and moment). In addition, maps of the flow field (vector plots) and vortex positions at prescribed time steps are available.

Flutter coefficients (aerodynamic derivatives) to be used as input in flutter routines and for determination of vortex-induced response are obtained by matching calculated time-dependent aerodynamic loads to forced vertical or rotational displacements in accordance with empirical models for self-excited aerodynamic loads. A similar method is used in wind and water tunnel applications [4]. As an alternative to forced motion simulations the cross-sections may be supported by theoretical springs, allowing direct simulation of the aeroelastic flow–structure interaction.

4. Bridge sections analysed

DVMFLOW simulations were carried out for four bridge girder cross-sections for which aerodynamic data were available from wind tunnel model tests. This provided a basis for comparison between numerical simulations and experiment. The bridge sections selected for analysis included:

- "H-shaped" plate section – 1st. Tacoma Narrows Bridge, 850 m main span suspension bridge, USA, 1940.
- "Semi-streamlined" mono-box section - Great Belt East Bridge, suspended spans of a 1624 m main span suspension bridge, currently under construction in Denmark [5].
- "Bluff" mono-box section – Great Belt East Bridge, 193 m multi span approaches leading up to the suspension bridge [6].
- "Semi-streamlined" twin-box section – Chain of 3550 m main span suspension bridges developed during a design study (APP) for a fixed link across the Straits of Gibraltar [10].

Impressions of the bridge structures and geometry of the girder cross-sections are presented in Figs. 1 and 2. Structural properties utilized in the analyses are summarized in Table 1.

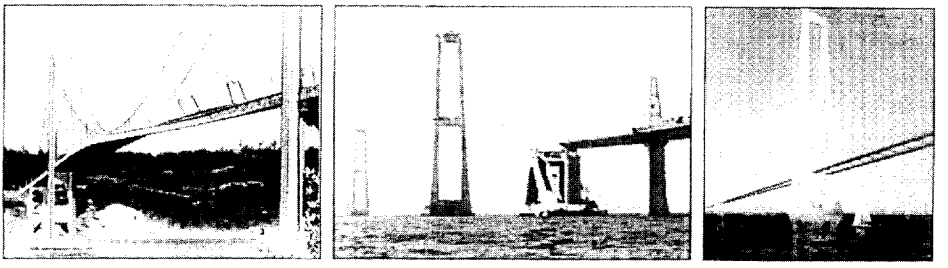

Fig. 1. View of bridges analysed. 1st. Tacoma Narrows Bridge (left), Great Belt East Bridge during construction, summer 1996 (middle) and the Gibraltar APP study artist's impression (right).

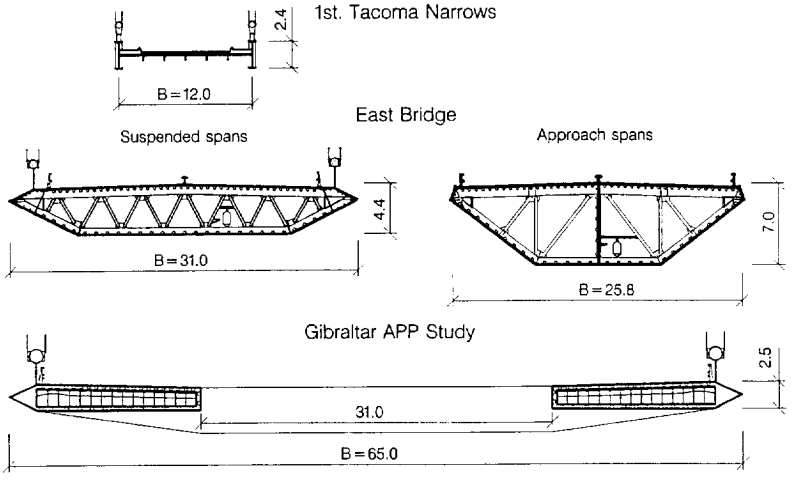

Fig. 2. Bridge girder cross-sections selected for DVMFLOW analysis.

Table 1
Structural properties of bridge cross-sections

Structural property	1st Tacoma Narrows	East Bridge Suspended spans	East Bridge approach spans	Gibraltar APP study
m (kg/m)	4.25×10^3	22.7×10^3	16×10^3	39.5×10^3
I (kgm^2/m)	177.73×10^3	2.47×10^6	1.05×10^6	26.7×10^6
f_h (Hz)	0.13	0.099	0.46	0.065
f_t (Hz)	0.20	0.272	2.76	0.093
ζ (rel-to-crit)	0.005	0.002	0.005	0.003

5. Results of flow simulations and comparison with wind tunnel tests

5.1. Drag coefficient and Strouhal number

DVMFLOW simulations were carried out for the four bridge girder cross-sections presented above. Objectives of these simulations were the assessment of the drag coefficient C_D and Strouhal number St at 0° angle of incidence. All simulations were carried out for stationary sections at Reynolds number $Re = 10^5$ based on cross-section width ($Re = UB/\nu$). All simulations on stationary sections were run for a non-dimensional time interval $0 < tU/B < 25$. Input panel models reproduced the large-scale geometry of the cross-sections (deck contour) but finer details such as railings and median dividers were omitted for the present analysis. Modification of DVMFLOW for modelling of such details is in progress.

Typical results of stationary simulations comprise plots of section aerodynamic drag coefficient $C_D = D/\frac{1}{2}\rho U^2 B$ (D is the drag load, B is the section width) and lift coefficient $C_L = L/\frac{1}{2}\rho U^2 B$ (L is the lift force) computed as function of the non-dimensional time tU/B. As an example $C_D(tU/B)$ and $C_L(tU/B)$ time traces obtained for the 1st Tacoma Narrows cross-section are presented in Fig. 3.

The steady-state drag coefficient C_D is obtained as the mean of the drag trace (Fig. 3, top). The Strouhal number, St, is obtained from the non-dimensional period TU/B for one oscillation of the lift coefficient (Fig. 3, bottom) scaled by section depth H: i.e. $St = (H/B)/(TU/B)$.

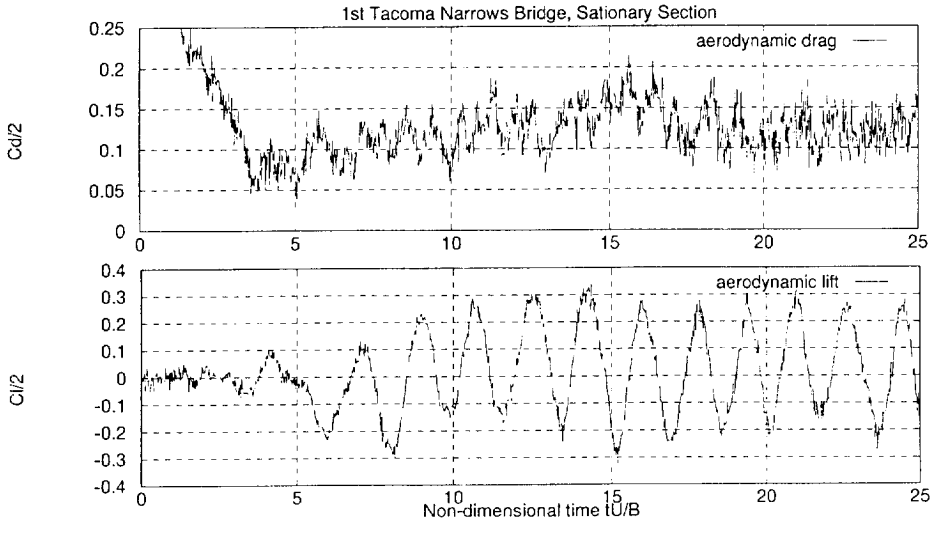

Fig. 3. Simulated time traces of aerodynamic drag (top trace, $C_D/2$ versus time) and lift (bottom trace $C_L/2$ versus time) for the 1st Tacoma Narrows cross-section.

Deck Section Geometry	DVMFLOW		Wind Tunnel	
	C_D	St	C_D	St
East Bridge, Suspension 	0.061	0.168 0.100	0.077	0.158 0.109
East Bridge, Approach 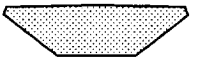	0.179	0.167	0.190	0.170
1st. Tacoma Narrows 	0.28	0.114	0.24 0.30	0.115
Gibraltar APP Study 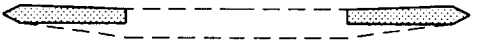	0.060	0.157 0.113	0.059	0.220

Fig. 4. Comparison of drag coefficient and Strouhal number obtained from numerical simulations and wind tunnel tests for four bridge girder cross-sections.

A summary of C_D, St and comparison with wind tunnel test results for the four cross-sections investigated are given in Fig. 4. It is noted that simulated and experimental C_D and St values agree very well for the two bluff sections, the East Bridge approach span [6] and 1st Tacoma Narrows cross-sections [7,8].

In the case of the cross-section of the East Bridge suspended spans, the C_D obtained from DVMFLOW simulations falls 20% below the value obtained from wind tunnel experiments [5]. A possible explanation for this discrepancy is that railings and median dividers were included in the wind tunnel model but omitted in the DVMFLOW panel model. Simple calculations allowing each of the railing components to be exposed to the free stream wind speed yield a drag contribution $\Delta C_D^{\text{railing}} = 0.023$. Hence, a total cross-section $C_D = 0.085$ which is 11% in excess of the C_D value obtained from wind tunnel tests.

A Fourier transform of the C_L time trace obtained for the suspended spans of the East Bridge displayed two vortex shedding frequencies. The main component St = 0.168 is in good agreement with St = 0.158 obtained from experiments with an elastically suspended section model. In the case of an elastically suspended section a slight decrease of the vortex frequency is expected due to motion-induced reduction of the apparent stiffness.

Vector plots of the simulated flow fields around the East Bridge cross-sections for the main and approach spans and the Gibraltar APP twin-deck are given in Fig. 5. The increased width of section wake and thus drag coefficient with increasing section bluffness is clearly recognized in the case of the East Bridge sections. The flow field around the Gibraltar twin-box cross-section indicates impingement and break up of vortices shed from the upwind girder element due to the presence of the down-wind girder element.

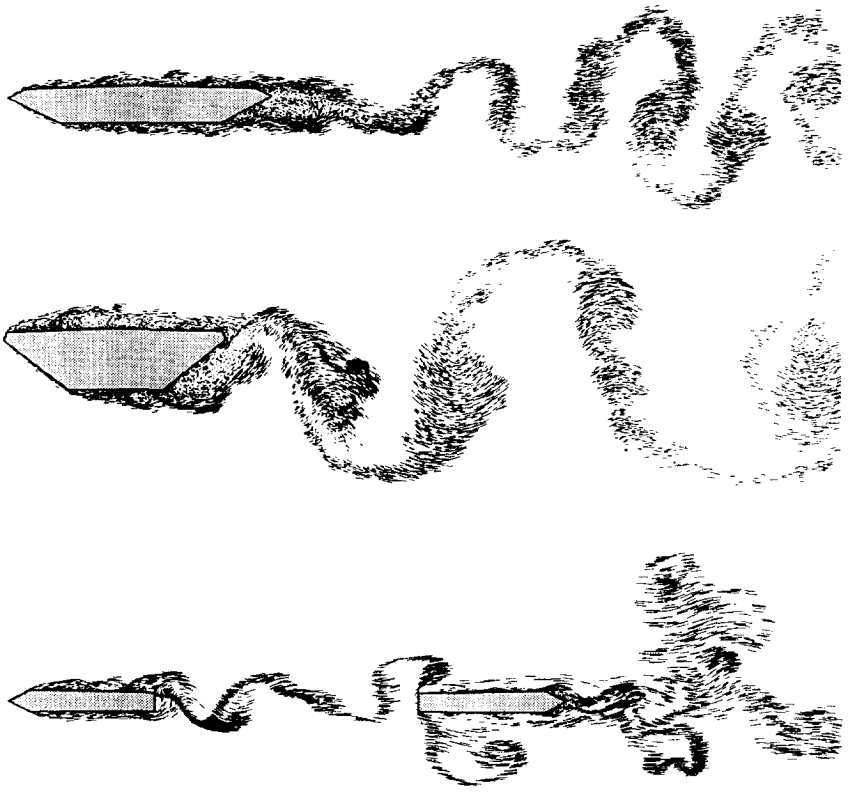

Fig. 5. Simulated flow fields around bridge girder cross-sections. Top: East Bridge suspended spans (shallow mono-box). Middle: East Bridge approach spans (deep mono-box). Bottom: Gibraltar APP twin-deck section.

5.2. *2DOF flutter*

2DOF (binary) flutter is encountered for flexible bridges with shallow "semi-streamlined" box girder cross-sections similar to the East Bridge and the Gibraltar APP study. For each of these cross-sections, forced motion simulations were carried out. The simulations involved separate oscillatory vertical and rotational motion about mid-chord for six reduced wind speeds in the interval $U/fB = 4$–14. Vertical amplitudes for the prescribed sinusoidal motion were taken to be $h/B = 0.04$ and $\alpha = 3.0°$–$5.0°$ for rotation about mid-chord. Typical results of forced oscillatory motion simulations comprise plots of section lift and moment coefficients C_L, C_M as function of non-dimensional time. As an example, $C_M(tU/B)$ traces obtained for the Gibraltar APP cross-section at reduced wind speeds $U/fB = 6$ and $U/fB = 12$ are shown in Fig. 6.

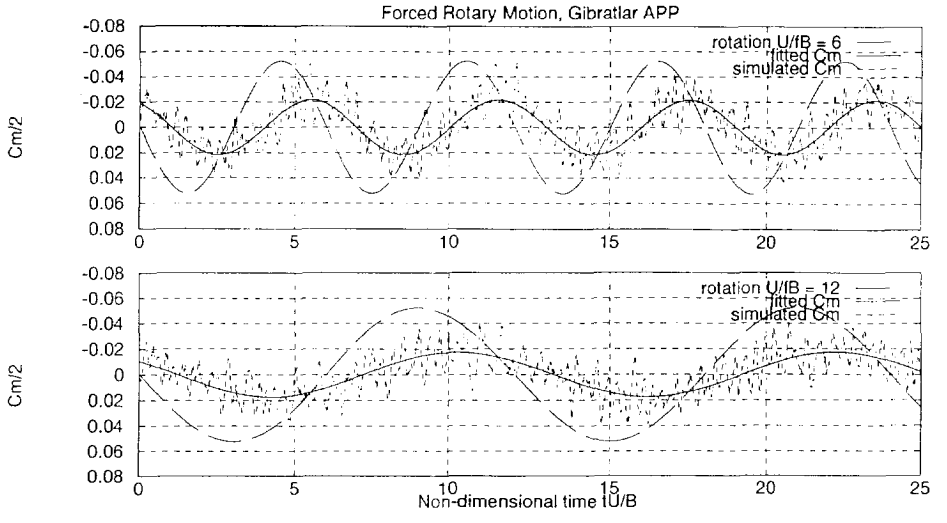

Fig. 6. Rotation and simulated and fitted time traces of aerodynamic moments (top: $C_M/2$ versus time at $U/fB = 6$, bottom: $C_M/2$ versus time for $U/fB = 12$). Gibraltar APP twin-box cross-section.

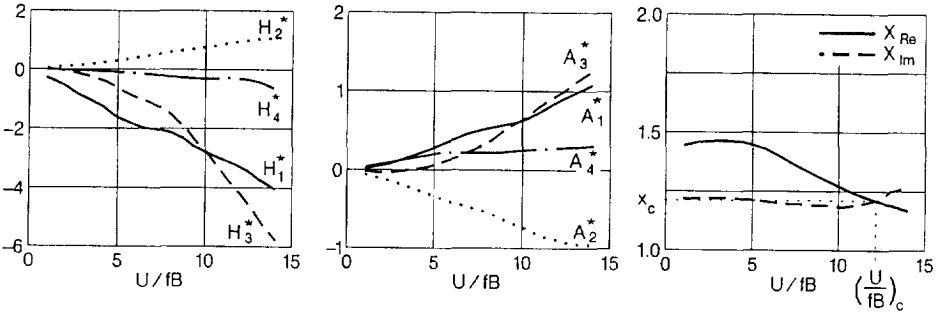

Fig. 7. Aerodynamic derivatives for the Gibraltar APP twin-box ($H^*_{1..4}$ left, $A^*_{1..4}$ middle) and intersection of the real and imaginary parts (X_{Re}, X_{Im}) of the corresponding flutter determinant defining the non-dimensional critical wind speed $(U/fB)_c$.

Simulated time traces of C_L, C_M appear as random narrow band oscillations (due to vortex shedding) modulated by the frequency of forced oscillation. The amplitudes of C_L, C_M at the forced excitation frequency are extracted by least-squares fitting of a sinusoid to the simulated load traces. The aerodynamic derivatives are obtained from the amplitude and phase relationship between the forced motion and the fitted load signals. The critical wind speed for onset of 2DOF flutter is obtained by combining structural properties with $H^*_{1..4}$, $A^*_{1..4}$ in the flutter determinant following the Theodorsen method of Simiu and Scanlan [2]. This procedure is illustrated in Fig. 7.

Deck Section Geometry	DVMFLOW U_C (m/s)	Wind Tunnel U_C (m/s)
East Bridge, Suspension 	74	73 [5]
Gibraltar APP Study 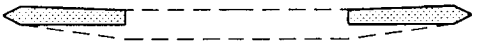	62	66 [10]

Fig. 8. Comparison of critical wind speeds obtained from DVMFLOW simulations and wind tunnel section model tests of the East Bridge suspension and Gibraltar APP girder cross-sections.

A comparison of prototype critical wind speeds U_c obtained from the DVMFLOW simulations and from wind tunnel section model tests of the East Bridge and Gibraltar APP cross sections is given in Fig. 8. Good to excellent agreement is noted indicating a maximum deviation between numerical simulations and wind tunnel tests of about 7%. Indeed satisfactory for design studies of long-span bridges.

5.3. *1DOF flutter*

1DOF (torsional) flutter is encountered for flexible bridges with channel type or H-shaped plate girder cross-sections. Forced motion simulations in pure rotation (deck torsion) were carried out for the 1st. Tacoma Narrows Bridge in order to test the ability of DVMFLOW to simulate the strongly non-linear and recirculating flow around this cross-section. The simulations involved three oscillation amplitudes $\alpha = 3°$, $10°$ and $30°$ and were carried out at reduced wind speeds in the range $U/fB = 2$–8. Fig. 9 compares the aerodynamic derivative A_2^* obtained from the DVMFLOW simulations to A_2^* given in Billah and Scanlan (Fig. 4) [9] for incipient torsional motion. The determination of corresponding critical reduced wind speeds $(U/fB)_c$ follows the method given by Simiu and Scanlan [2], detailed in Ref. [9] and further illustrated in Fig. 9 (left). Fig. 9 (right) compares predicted prototype torsional responses to results of the full 3-D aeroelastic wind tunnel tests of the 1st. Tacoma Narrows Bridge carried out by Farquharson [8]. The predictions assume a structural damping $\zeta = 0.005$ (rel-to-crit) as reported for the full bridge model test. Fair agreement is demonstrated for torsional motion amplitudes $\alpha = 3°$ and $10°$ although the DVMFLOW simulations yield higher wind speeds for similar response as compared to the full bridge model tests.

The prototype bridge collapsed in a 19 m/s gale on 7 November 1940, while twisting at amplitudes of approximately $\alpha = 30°$–$35°$. A full-scale wind speed of 19 m/s corresponds to a reduced wind speed $(U/fB)_c = 7.9$ which by virtue of Fig. 9 (left) corresponds to a critical aerodynamic derivative $(A_2^*)_c = 0.2$. Introducing the relevant mass moment of inertia and torsional frequency (Table 1) in the $(A_2^*)_c$-relation $((A_2^*)_c = 2I\zeta/\rho B^4)$ yields a relative structural damping $\zeta = 0.014$ (rel-to-crit) at the

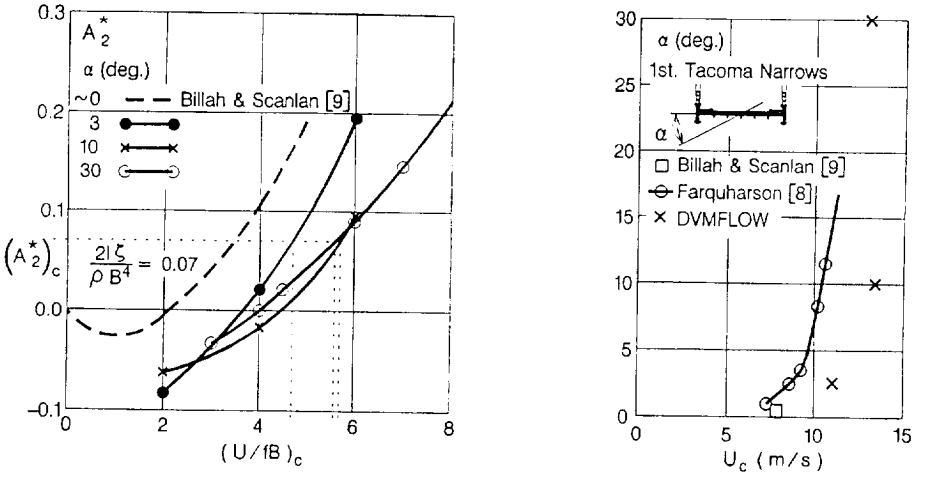

Fig. 9. A_2^* aerodynamic derivative (left) and predicted prototype torsional response (right) obtained from DVMFLOW forced simulations of the 1st. Tacoma Narrows Bridge cross-section.

stage of collapse. This damping level is high compared to $\zeta = 0.005$ but may well be realistic when considering cracking of the concrete deck. Codes of practice yield $\zeta = 0.016$ as typical for reinforced but not pre-stressed concrete structures.

The simulated flow field around the 1st. Tacoma Narrows Bridge cross-section during half a circle of oscillation is shown in Fig. 10. The reduced wind speed is $U/fB = 8$ and the amplitude of twisting motion is $\alpha = 30°$. Heavily recirculating flow below the deck and roll up of a strong leading edge vortex above the deck is evident.

The vortex pattern developing in Fig. 10 resembles the heuristic sketch by Billah and Scanlan [9], Fig. 6.

5.4. *Vortex-induced response*

Plate- as well as deep box-type cross-sections are known to be prone to vortex-induced oscillations at wind speeds where vortex shedding locks on to a structural eigenfrequency.

In practice, vertical oscillations are usually found to be the most important type of response as vertical eigenfrequencies of bridges tend to be lower than torsional eigenfrequencies. The ability of DVMFLOW to predict vertical vortex-induced oscillations of bridge girders was investigated in two cases, the 1st. Tacoma Narrows Bridge and the East Bridge approach span cross-sections.

Forced vertical motion simulations were run at reduced wind speeds bracketing the Strouhal number obtained from flow simulations on the stationary sections. In the case of the 1st. Tacoma Narrows cross-section a Strouhal number $St = 0.114$ was obtained from flow simulations reported in Section 5.1. Aerodynamic vortex shedding excitation was thus anticipated at $U/fB = 1.8$. Forced motion simulations were run in

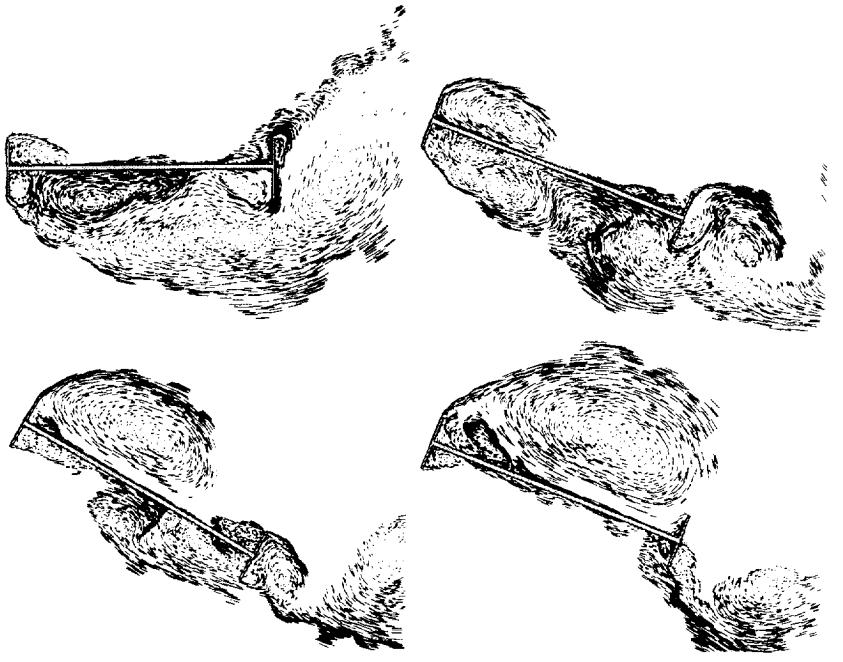

Fig. 10. Simulated flow around the 1st. Tacoma Narrows Bridge twisting at 30° amplitude.

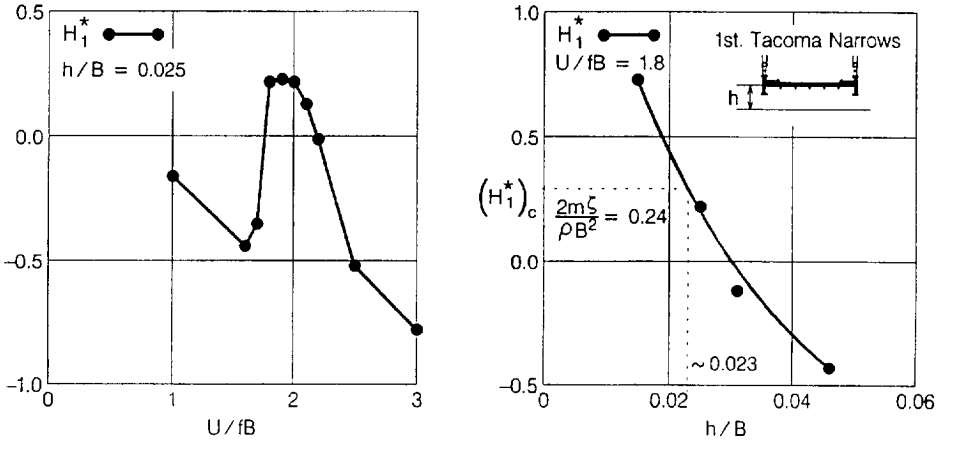

Fig. 11. H_1^* aerodynamic derivative (left) and predicted prototype vertical response (right), 1st. Tacoma Narrows cross-section.

the range $U/fB = 1$–3 and at a constant amplitude $h/B = 0.025$. The results displayed a pronounced shift of the polarity of the H_1^* aerodynamic derivative (from − to +) in the vicinity of $U/fB = 1.8$ as expected, Fig. 11 (left). Simulations proceeded at $U/fB = 1.8$ but at varying amplitudes in the range $h/B = 0.015$–0.045. A stationary

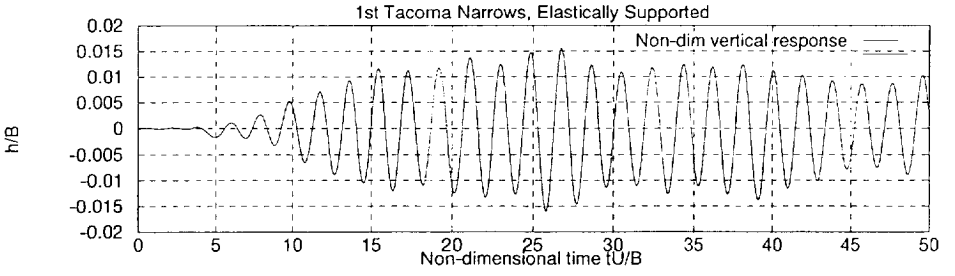

Fig. 12. Simulated vertical response of the elastically suspended 1st. Tacoma Narrows section.

Deck Section Geometry	Mode of Motion	DVMFLOW		Wind Tunnel	
		h/B	St	h/B	St
1st. Tacoma Narrows	Forced Oscillation	0.023	0.11	–	–
h Model scale : *1:50 **1:36	Elastic Suspension	0.020	0.11	* 0.024 [8] ** 0.040	* 0.09 [8] ** 0.12
East Bridge, Approach h	Elastic Suspension	0.014	0.16	0.021 [6]	0.16 [6]

Fig. 13. Comparison of vertical vortex-induced response obtained from DVMFLOW simulations and wind tunnel tests with the 1st. Tacoma Narrows and East Bridge approach sections.

vortex-induced amplitude $h/B = 0.023$ was obtained by balancing aerodynamic vortex shedding excitation and dissipation of energy by structural damping, Fig. 11 (right). A structural damping level $\zeta = 0.005$ (rel-to-crit) was assumed.

Simulation of flow–structure interaction on elastically suspended cross-sections is a distinct alternative to forced oscillation runs as discussed above. This type of simulation requires that the flow problem and the 1DOF equation of vertical section motion are solved simultaneously. Similarity considerations yield identical mass ratio $\rho B^2/m$ for computer model and prototype. Hence resonance at the Strouhal frequency fixes the spring constant in the equation of motion as $k = (2\pi \mathrm{St} U/H)^2/(m/\rho)$. The simulated elastic h/B response versus non-dimensional time obtained for the 1st. Tacoma Narrows cross-section is shown in Fig. 12.

From Fig. 12 it is noted that the stationary vertical response obtained from the simulation of the elastically suspended cross-section is in qualitative agreement with the vertical response obtained from the forced-response simulations.

A comparison of the prototype of vertical vortex-induced response and Strouhal number obtained from DVMFLOW simulations and wind tunnel tests for the 1st. Tacoma Narrows Bridge and the East Bridge approach cross-sections is given in Fig. 13. Satisfactory agreement is demonstrated.

Acknowledgements

The continuing encouragement of colleagues of the COWI bridge department and the financial support of the COWI foundation is highly appreciated.

References

[1] J.H. Walther, A. Larsen, 2D Discrete vortex method for application to bluff body aerodynamics, These Proceedings, J. Wind Eng. Ind. Aerodyn. 67&68 (1997) 183–193.
[2] E. Simiu, R.H. Scanlan, Wind Effects on Stuctures, 2nd ed., Wiley Interscience, New York, 1986.
[3] J.H. Walther, Discrete vortex method for two-dimensional flow past bodies of arbitrary shape undergoing prescribed rotary and translatory motion, AFM-94-11, Ph.D. Thesis, Department of Fluid Mechanics, Technical University of Denmark, 1994.
[4] Q.C. Li, Measuring flutter derivatives for bridge sectional models in water channel, ASCE J. Mech. Eng. 121 (1) (1995) 90–101.
[5] A. Larsen, JWEIA Aerodynamic aspects of the final design of the 1624 m suspension bridge across the great belt, J. Wind Eng. Ind. Aerodyn. 48 (1993) 261–285.
[6] DMI report No. 92194.01: Detailed design, approach bridges, section model tests III, Storebælt East Bridge, March 1993, Restricted.
[7] G. Schewe, Nonlinear flow-induced resonances of an H-shaped section, J. Fluids Struct. 3 (1989) 327–348.
[8] F.B. Farquharson, Aerodynamic stability of suspension bridges, University of Washington Experiment Station, Bull. No. 116, Part I and III, 1952.
[9] K.Y. Billah, R.H. Scanlan, Resonance, Tacoma Narrows bridge failure, and undergraduate physics textbooks, Amer. J. Phys. 59 (2) (1991) 118–124.
[10] A. Larsen, K.H. Ostenfeld, M. Astiz, Aeroelastic stability study for the Gibraltar bridge feasibility phase, IV Int. Coll. Gibraltar Fixed Link, Seville 1995, pp. 273–278.